

Evidence for the Rate of the Final Step in the Bacteriorhodopsin Photocycle Being Controlled by the Proton Release Group: R134H Mutant[†]

Miao Lu,[‡] Sergei P. Balashov,[‡] Thomas G. Ebrey,^{*,‡} Ning Chen,[§] Yumei Chen,[§] Donald R. Menick,[§] and Rosalie K. Crouch[§]

Center for Biophysics and Computational Biology and Departments of Cell and Structural Biology, and Biochemistry, University of Illinois at Urbana-Champaign, Urbana, Illinois 61801, and Medical University of South Carolina, Charleston, South Carolina 29425

Received November 4, 1999; Revised Manuscript Received December 27, 1999

ABSTRACT: Light absorbed by bacteriorhodopsin (bR) leads to a proton being released at the extracellular surface of the purple membrane. Structural studies as well as studies of mutants of bR indicate that several groups form a pathway for proton transfer from the Schiff base to the extracellular surface. These groups include D85, R82, E204, E194, and water molecules. Other residues may be important in tuning the initial state pK_a values of these groups and in mediating light-induced changes of the pK_a values. A potentially important residue is R134: it is located close to E194 and might interact electrostatically to affect the pK_a of E194 and light-induced proton release. In this study we investigated effects of the substitution of R134 with a histidine on light-induced proton release and on the photocycle transitions associated with proton transfer. By measuring the light-induced absorption changes versus pH, we found that the R134H mutation results in an increase in the pK_a of the proton release group in both the M (0.6 pK unit) and O (0.7 pK unit) intermediate states. This indicates the importance of R134 in tuning the pK_a of the group that, at neutral and high pH, releases the proton upon M formation (fast proton release) and that, at low pH, releases the proton simultaneously with O decay (slow proton release). The higher pK_a of the proton release group found in R134H correlates with the slowing of the rate of the O \rightarrow bR transition at low pH and probably is the cause of this slowing. The pH dependence of the fraction of the O intermediate is altered in R134H compared to the WT but is similar to that in the E194D mutant: a very small amount of O is present at neutral pH, but the fraction of O increases greatly upon decreasing the pH. These results provide further support for the hypothesis that the O \rightarrow bR transition is controlled by the rate of deprotonation of the proton release group. These data also provide further evidence for the importance of the R134–E194 interaction in modulating proton release from D85 after light has led to its being protonated.

Bacteriorhodopsin (bR),¹ a seven-transmembrane-helix protein found in the purple membrane of *Halobacterium salinarum*, contains a retinal chromophore attached to the apoprotein via a protonated Schiff base linkage. Upon absorption of a photon, the all-trans retinal isomerizes to its 13-cis configuration, initiating a photocycle that is coupled to vectorial proton transport from the cytoplasmic to the extracellular side of the membrane. The photocycle is characterized by a series of distinct photointermediates, named J, K, L, M, N, and O (reviewed in refs 1–4).

During the L \rightarrow M transition, a proton is transferred from the Schiff base to D85, driven by changes of the proton affinities of these two residues induced by the chromophore photoisomerization. Near neutral pH, this process coincides

with a proton being released from the proton release group (PRG) that includes residues E204 (5–7) and E194 (8–9), assembled in a hydrogen-bonded network (10–12), to the extracellular surface of the membrane. This light-induced proton release (usually called “early” or “fast” proton release) occurs with $\tau_e \approx 80 \mu\text{s}$ in the WT. The time constant is determined by experiments with pH-sensitive dyes (13–15) or photocurrents from oriented samples (16). During the M \rightarrow N transition, the Schiff base is reprotonated from D96 located at the cytoplasmic side of the membrane. The early proton release seen near neutral pH is followed by a slower uptake of a proton from the cytoplasmic side with $\tau_e \approx 5 \text{ ms}$, coincident with the N \rightarrow O transition. This reprotonation of D96 from the cytoplasmic surface is accompanied by reisomerization of the retinal chromophore (4). D85 remains protonated until the end of the photocycle, and during the O \rightarrow bR transition, a proton from D85 is transferred to the PRG, thus resetting the initial state of D85 and the PRG (6, 17). In the lower pH range (pH < pK_a of PRG in M), proton release (“late” proton release) is delayed to the end of the photocycle, and occurs during the O \rightarrow bR transition (18–19).

[†] This work was supported by NIH Grant GM52023 (to T.G.E.) and DOE Grant 95ER20171 (to R.K.C.).

^{*} To whom correspondence should be addressed. Present address: Box 351330, University of Washington, Seattle, WA 98195. Phone: (206) 685-3550. Fax: (206) 543-3262. E-mail: t-ebrey@uiuc.edu.

[‡] University of Illinois at Urbana-Champaign.

[§] Medical University of South Carolina.

¹ Abbreviations: bR, bacteriorhodopsin; WT, wild type; DA, dark adaptation; k_{da} , the rate constant of dark adaptation; PRG, proton release group.

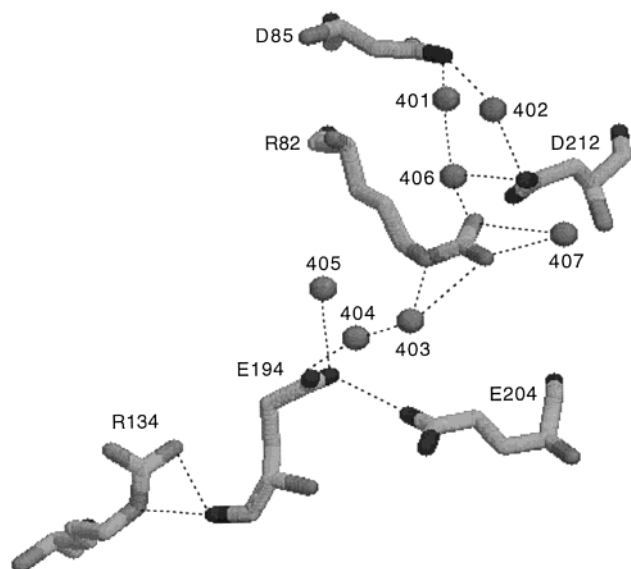


FIGURE 1: Extracellular region of bacteriorhodopsin based on the most recent structure by Luecke et al. (11). Hydrogen bonds are drawn as dashed lines. Water molecules are numbered from 401 to 407. The distance between R134 and E194 polar side groups is 5.3 Å.

Mutation of R82 (20), E204 (5), or E194 (8, 9) inhibits or completely abolishes the fast proton release. R82 moves toward the extracellular surface during the L \rightarrow M transition (12), presumably causing the PRG to deprotonate. E194 and E204 are essential for the fast proton release. Another residue that might be important in this proton-transfer process is R134 (21), which is located on the extracellular side of the membrane (11, 22–25).

The goal of this study is to perturb interactions of R134 by observing the consequences of the R134H mutation and thus elucidate the functional role of R134 in bR. R134 is conserved in all halobacterial retinal proteins that have been sequenced so far, including halorhodopsin and sensory rhodopsins. According to structural studies (11, 22–25) R134 is located close to the extracellular surface in helix E and near E194. In the most recent X-ray structure of Luecke et al. (11), the distance between their charged groups is 5.3 Å, and R134 forms two hydrogen bonds with the peptide carboxyl of E194 (Figure 1). It is reasonable to suggest that interaction with positively charged R134 may decrease the pK_a of the nearby carboxyl groups, primarily that of E194, by stabilizing the ionized state of this group due to direct electrostatic interaction and/or through hydrogen bonding, thus affecting the pK_a of the PRG. A study of the R134K mutant (21) provided the first evidence that this indeed takes place. Several changes were induced by the R134K mutation. In the ground state, the pK_a of the PRG was decreased from 9.7 to 8.0, while the pK_a of D85 was increased from 2.6 to 4.6. We call the magnitude of the change in the pK_a of one of the two interacting groups upon a change of the protonation state of the other group the *coupling strength* (27). The coupling strength of D85 with the PRG was reduced from 4.8 pK units in the WT (26–27) to 3.0 in the R134K mutant, and the pH dependence of light-induced proton release kinetics during M formation was altered (21).

Recently Balashov et al. (27) presented evidence that the pK_a of the PRG in the O intermediate is a key factor in controlling the rate of recovery of bR in the O \rightarrow bR

transition at low pH. We also showed that the relatively conservative mutation of E194D causes a 1 pK unit increase in the pK_a of the PRG in O. If the interaction of the PRG with R134 is important, then a perturbation of this interaction by replacing arginine with a histidine should result in a similar shift of the pK_a of E194 and the pK_a of the PRG in the M and O intermediates. Like arginine, histidine is positively charged at low pH, but with a shorter side chain, so one would expect to see a weakening of the E194–H134 interaction and an increase in the pK_a of E194. If the protonation state of E194 affects proton release from D85, then changes in the pK_a of this group should also result in an altered pH dependence of O decay. If a weak coupling exists between D85 and E194, as our data on the E194D mutant imply (27), then one may also expect to see an altered titration for D85 and therefore an altered pH dependence of dark adaptation.

In this study we examined these predictions for the R134H mutant. We found that in R134H the pH dependence of the yield of O is altered in a way similar to that in the E194D mutant, and that the pK_a of the PRG in the M and O intermediates in R134H is about 0.7 pK unit higher than that in the WT. This provides further evidence that R134 is involved in controlling the pK_a of the PRG. We also found that the R134H mutation affects the titration of D85.

MATERIALS AND METHODS

Site-directed mutagenesis of bR, the transformation of the R134 mutants in *H. salinarium* strain IV-8, and the preparation of the purple membrane followed procedures described earlier (20, 28). The absorption spectra were recorded using a Cary-Aviv 14DS spectrophotometer (Aviv Associates, Lakewood, NJ). Flash-induced transient absorbance changes were measured with a home-built kinetic spectrophotometer (29). Actinic flashes at 532 nm were provided by a Quanta Ray DCR-11 Nd:YAG laser (Spectra-Physics, Mountain View, CA). The optical density of the samples for flash-induced absorption change measurements was 0.4–0.5 at 568 nm. Light-induced proton release and uptake were measured with the pH-sensitive dye pyranine. The pK_a of pyranine is 7.2 in 150 mM KCl. The absorbance change of the dye was obtained by subtracting the kinetics traces at 460 nm with and without dye. Kinetic traces were obtained by averaging signals from 32 to 64 flashes. Acrylamide gels were used to prevent the aggregation and sedimentation of the pigment at low pH values. The gels were incubated overnight at a given pH (26). Light adaptation was carried out by illumination with a 500 W projector ($\lambda = 430$ –550 nm) for 5 min. The rate of dark adaptation was followed by the absorbance decrease at 580 nm (26). Kinetics analysis of the traces was performed using the KaleidaGraph software package (Synergy Software, Reading, PA). All the measurements were performed in 75 mM K_2SO_4 or 150 mM KCl at 20 °C. A mixture of six buffers (citric acid, Mes, Hepes, Mops, Ches, Caps) was used to maintain the pH between 2 and 11 as described earlier (26).

RESULTS

To characterize the effect of the R134H mutation on the function of bR, we studied pH dependencies of the absorption spectrum and the rate constant of thermal isomerization, the

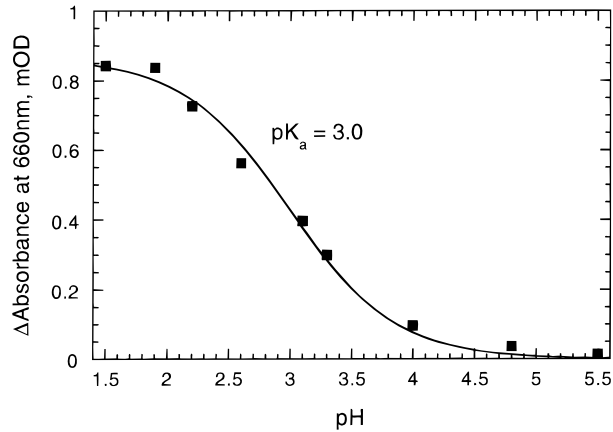


FIGURE 2: pH dependence of the absorption changes at 660 nm caused by the purple-to-blue transition in R134H upon decreasing pH. The titration was performed on dark-adapted samples in 75 mM K₂SO₄ at 20 °C. The curve is the fit as a $n = 1$ transition with a pK_a of 3.0.

Table 1: pK_a of the PRG X and D85 in Different States of the Pigment

pigment	X in M	X in O	X in BM ^a	X in PM ^a	D85 (XH) ^b	D85 (X ⁻) ^c
WT	5.7 ^d	4.3	4.8	9.7 ^e /9.2 ^f	2.6	7.5 ^f
R134H	6.3	5.0	5.5	9.8 ^e /8.7 ^f	2.9	7.2 ^f

^a BM and PM, blue membrane and purple membrane, correspondingly. ^b pK_a of D85 in bR when X is protonated. ^c pK_a of D85 in bR when X is deprotonated. ^d Taken from ref 19. ^e Determined from the dark adaptation experiments, Figure 4 for R134H and ref 26 for the WT. ^f Determined from the pH dependence of the formation of the M intermediate, Figure 5 for R134H and ref 33 for the WT.

kinetics of the late photocycle intermediates, and the light-induced proton uptake and release process. The pK_a of D85 in the unphotolyzed state of R134H was determined by both titration of the purple-to-blue membrane transition and the pH dependence of the rate constant of dark adaptation (26). The pK_a of the PRG in the ground state was estimated from the pH dependence of dark adaptation (26, 28), of its partial transformation into the P480 species (30), and of the rate constant and fraction of the fast component of M formation (21, 28) as described below. The pK_a of the PRG in M is estimated from the pH dependence of the fast component of proton release (19). The pK_a of the PRG in O was inferred from the pH dependence of the rate constant of O decay as suggested by Balashov et al. (27).

Effect of the R134H Mutation on the Purple-to-Blue Transition (pK_a of D85). Decreasing the pH from 6.9 to 1.5 causes a shift in the absorption maximum of dark-adapted R134H from 561 to 603 nm due to the purple-to-blue transition associated with protonation of D85 (31–32). A plot of the absorbance changes at 660 nm (which are proportional to the fraction of blue membrane and therefore the fraction of protonated D85) versus pH gives a titration curve for D85, which can be best fitted with a pK_a of 3.0 ($n = 1$) in the pH range between 5.5 and 1.5 (Figure 2). This result differs from that obtained for the WT in which the titration curve of the purple to blue transition shows a pK_a of 2.6 ($n = 1.6$) in this pH range (see Table 1).

Partial Transformation of bR into P480 at High pH. Increasing the pH from 7 to 11 shifts the absorbance maximum of the pigment to shorter wavelengths, due to the formation of the P480 species (33). We plotted the absor-

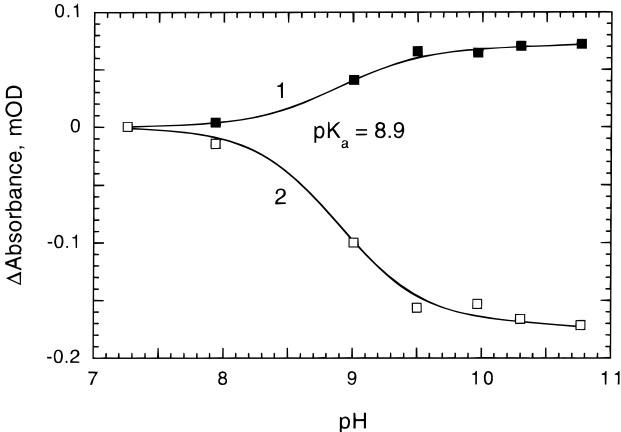


FIGURE 3: pH dependence of the absorption changes at 470 nm (1) and 580 nm (2) in R134H upon increasing pH. The titration was performed on dark-adapted samples in 75 mM K₂SO₄ at 20 °C. The curves are fits with a pK_a of 8.9, $n = 1$.

bance changes at two wavelengths, 470 nm, which reflects P480 formation, and 580 nm, which is due to the decrease in the amount of bR initially present. Both curves can be fitted with a pK_a of 8.9 (see Table 1 and Figure 3), which probably reflects the pK_a of the PRG in the unphotolyzed pigment as suggested by Govindjee et al. (30). Deprotonation of the PRG may be coupled to some other process, causing formation of P480 at higher pH (pH > 11). Because of this complication, the pK_a of the partial transformation of the pigment into P480 may be shifted by another transition, and therefore may not necessarily coincide exactly with the pK_a of the PRG.

pH Dependence of the Rate Constant of Dark Adaptation in R134H Indicates an Elevated pK_a of the PRG upon Protonation of D85. Important information on the coupling of D85 with the PRG, including the pK_a of the PRG, can be inferred from the pH dependence of the rate constant of dark adaptation, k_{da} (26, 28). k_{da} is proportional to the fraction of the blue membrane, f_{bm} (20, 26), and can readily be measured over a wide pH range. The rate constant of dark adaptation, k_{da} , was obtained from the time course of the absorption changes at 585 nm in the dark immediately after green light illumination to light adapt the sample. Above pH 5 the kinetics of DA are monoexponential so that the rate constant can be easily determined and plotted as a function of pH (Figure 4). Below pH 5.5, k_{da} increases upon decreasing the pH with a pK_a of 2.9, similar to the pK_a of the main purple-to-blue transition. Comparison of the pH dependence of k_{da} (squares) with the fraction of the blue membrane, f_{BM} , (circles), shows that k_{da} approximately follows the f_{BM} (Figure 4), which implies that thermal isomerization occurs via the blue membrane formed on transient protonation of D85 (20, 26).

Between pH 6 and pH 9 the rate constant of dark adaptation in R134H is almost constant; it is 2 times smaller than the rate in the WT. The plateau in the pH dependence of dark adaptation originates from the complex titration of D85 (26) due to coupling of its pK_a with the pK_a of the PRG. The point where the plateau approximately starts corresponds to the pK_a of the PRG in the state when D85 is protonated (i.e., for the blue membrane). In the case of R134H this pK_a is 5.5, as determined by a fit of the data with the model of two interacting residues; this is 0.7 pK unit higher than in

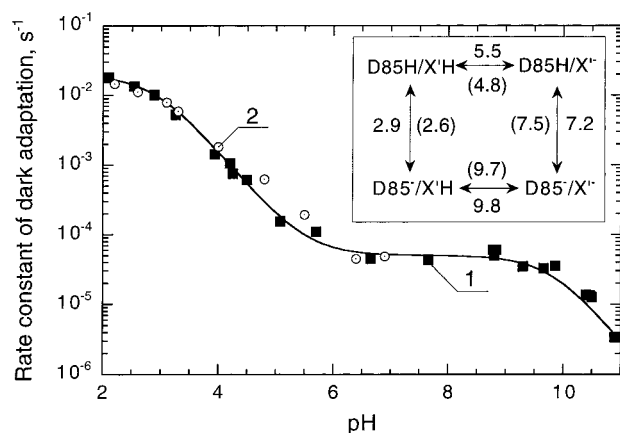


FIGURE 4: (1) pH dependence of the rate constant of thermal all-trans \rightarrow 13-cis isomerization (dark adaptation) in R134H at 20 °C. The curve is the fit of the pH dependence of k_{da} with the model of two interacting residues, D85 and the PRG (26). The protonation state of each group alters the pK_a of the other group, leading to the complex titration curve. The pK_a values of the fit are given in the inset. Values in parentheses are for the WT. (2) Acid titration of the R134H mutant. Data were normalized to compare with the rate constant of dark adaptation. As suggested in refs 26 and 28, X' and the proton release group X (19) are the same complex of residues.

the WT (4.8) (26). At high pH, k_{da} decreases in R134H with a pK_a around 9.8, close to that in the WT. This transition presumably reflects deprotonation of the PRG in the ground state as also seen in the WT (26).

pH Dependence of M Formation in R134H. The kinetics of formation of the M intermediate are biphasic in R134H. Both the rate constants (Figure 5A) and amplitudes (Figure 5B) of the two components are pH dependent. As in the WT, the formation of the M intermediate speeds up as the pH increases (Figure 5A) but to a lesser extent than that in the WT (16, 33). The rise time of the fast component is about 5 μ s at pH > 7 in R134H, and increases to 12 μ s at low pH with a pK_a of 6.0. This value is close to the pK_a of the PRG in M (see below). The fraction of the fast component comprises about 15% of the amplitude in the pH range 4–8 but increases up to 70% at pH 10, with a pK_a of 8.7 (Figure 5B). A similar increase is observed in the WT with a pK_a of 9.2 (16, 33). The change in kinetics was attributed to an increase in the pK_a of D85 caused by deprotonation of the PRG in the ground state as the pH increased (26, 28). Thus, the transition with a pK_a of 8.7 in R134H is probably related to the deprotonation of the PRG in the unphotolyzed state of R134H. The rise time of the slow component is 80 μ s at pH < 8, but it speeds up to 15 μ s at pH 10 with a pK_a of 9.7 (Figure 5A), which also may be related to the deprotonation of the PRG.

pH Dependence of Formation and Decay of O in R134H. Light-induced absorption changes at 660 nm due to formation and decay of the O intermediate together with the absorption changes at 410 and 580 nm are shown in Figure 6 at two pH values: 6.9 and 3.0. One can see that at pH 6.9 (Figure 6A) the fraction of O is very small, but increases greatly at low pH (Figure 6B). The increase in the fraction of O is accompanied by an increase in the lifetime of O (Figure 6C). This is similar to what is seen in the WT, in which the amount of O increases at low pH while the decay of O slows down (27). However, the pH dependence of the fraction of

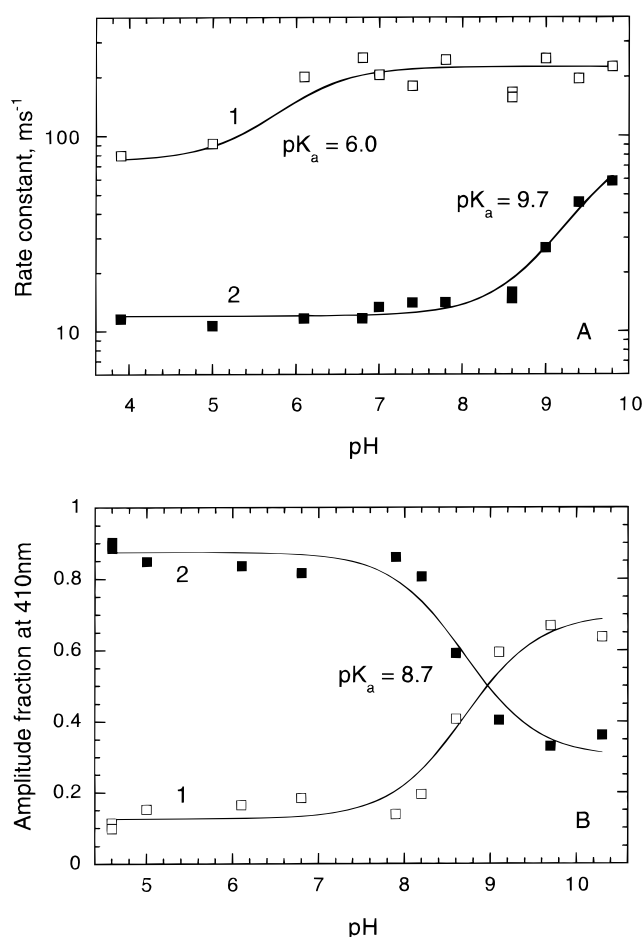


FIGURE 5: (A) pH dependence of the apparent rate constants of M formation in R134H: 1, fast component; 2, slow component. (B) pH dependence of the fractions of the M intermediate in R134H: 1, fast component; 2, slow component.

O (Figure 7A) and the pH dependence of the rate constant of O decay (Figure 7B) are substantially altered compared to those of the WT. As one can see from Figure 7A, at neutral pH, a much smaller amount of O is observed in R134H than in the WT (compare curves 1 and 2). The fraction of O decreases with a pK_a of 6.4 versus 7.5 in the WT. At lower pH values, the amplitude of O increases with a pK_a of 4.1.

The pH dependence of the apparent rate constants of O rise and O decay are shown in Figure 7B. The data were analyzed using a simplified kinetic model for the last segment of the photocycle $M \rightarrow N \rightleftharpoons O \rightarrow bR$ as described earlier (27). The curves show the assignment of the experimental (apparent) rate constants to the rate constants of the $N \rightarrow O$ (curve 1) and $O \rightarrow bR$ (curve 2) transitions, respectively. The apparent rate constant, which at pH 6 appears as O rise, is attributed to the rate constant of the $O \rightarrow bR$ transition. This rate constant decreases more than 25-fold with a pK_a of 5.0 upon decreasing the pH to 3 (from 250 to 10 s^{-1}). In the WT a similar decrease occurs with a pK_a of 4.3 (curve 3, Table 1, and ref 27). Balashov et al. (27) suggested that the rate of the $O \rightarrow bR$ transition at low pH is controlled by the deprotonation of the PRG. Therefore, the result above indicates that the pK_a of the PRG in O is ca. 5.0 in R134H, about 0.7 pK unit higher than that in the WT (27). The rate constant of O formation is almost pH independent below pH 7. This assignment of the rate constants explains the large increase in the fraction of the O intermediate at pH below 5

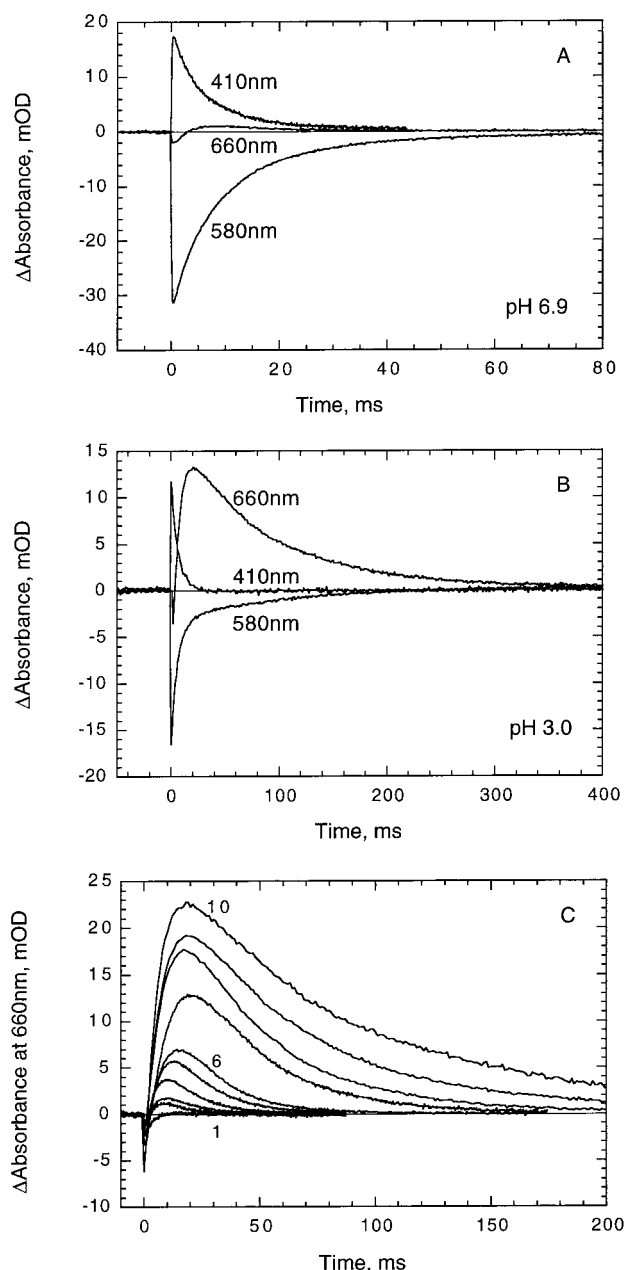


FIGURE 6: (A) Kinetics of the absorption changes at 410, 580, and 660 nm in R134H at pH 6.9. (B) Kinetics of the absorption changes at 410, 580, and 660 nm in R134H at pH 3.0. (C) Light-induced absorbance changes at 660 nm in R134H (caused by formation and decay of the O intermediate) at different pH values: traces 1–10 were taken at pH 7.9, 6.8, 6.0, 5.5, 5.0, 4.6, 4.2, 3.8, 3.4, and 3.0.

with a pK_a of 4.1 (curve 1 in Figure 7A). It should be mentioned that the maximum apparent rate constant of O rise (250 s^{-1} at pH 6–7) is close to the rate constant of the fast component of the $M \rightarrow N$ transition ($300 \pm 50 \text{ s}^{-1}$) and may be limited by this transition. The actual rate constant of the $O \rightarrow bR$ transition at pH 6–7 may be even larger than 250 s^{-1} .

Light-Induced Proton Release and Uptake in R134H. The kinetics of light-induced proton release and uptake in R134H was followed with the pH-sensitive dye pyranine (Figure 8). A decrease of absorbance corresponds to proton release. At pH 7 only fast proton release followed by proton uptake is observed, whereas at pH 6 the phase of fast proton release is not readily observable and mainly slow proton release,

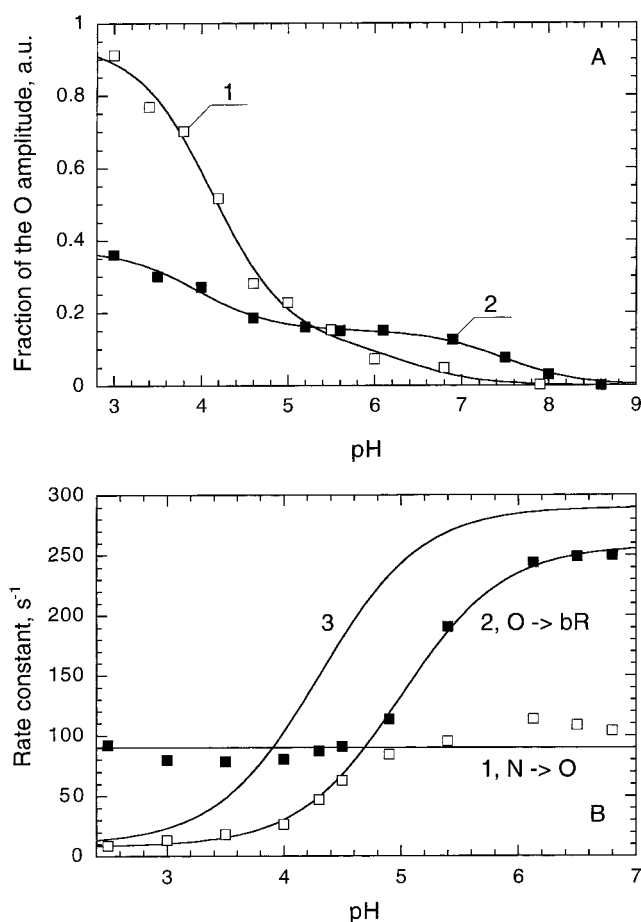


FIGURE 7: (A) pH dependence of the relative fraction of the O intermediate (maximum light-induced absorption change at 660 nm due to the formation of the O intermediate divided by maximum absorption change at 410 nm due to the M intermediate) in R134H (curve 1) and the WT (curve 2). The curve for R134H could be fit with two pK_a values of 4.1 and 6.4. The curve for the WT can be fit with two pK_a values of 3.9 and 7.5. (B) pH dependence of the apparent rate constants of O formation (closed squares) and O decay (open squares). Lines show the assignment of the experimental rate constants to the rate constants of the $N \rightarrow O$ (1) and $O \rightarrow bR$ transitions (pK_a of 5.0) (2), as was proposed for the WT (27). This assignment enables us to simulate the pH dependence of the fraction of O (Figure 7A) using the formula derived in ref 27. (3) pH dependence of the rate constants of the $O \rightarrow bR$ transition in the WT (pK_a 4.3), taken from ref 27.

here preceded by proton uptake, is seen. The fraction of fast proton release decreases upon decreasing the pH with a pK_a of about 6.3, which probably represents the pK_a of the PRG in M (19). Below this pH, the PRG cannot deprotonate after M is formed, but it will deprotonate, on a slower time scale, during the $O \rightarrow bR$ transition with a lower pK_a of 5.0. In the WT, the pK_a of the PRG in M was estimated to be 5.7 (19). Thus, the R134H mutation results in an increase of the pK_a of the PRG in M by about 0.6 pK units indicating this mutation affects the pK_a of the PRG presumably through alteration of electrostatic interactions. At pH 6 the apparent rate constant of O decay almost coincides with the proton release. At pH 6.8 the apparent rate constant of the O decay is close to the rate of proton uptake, which apparently is the rate-limiting step at this pH.

DISCUSSION

Estimations of the pK_a of the Proton Release Group in

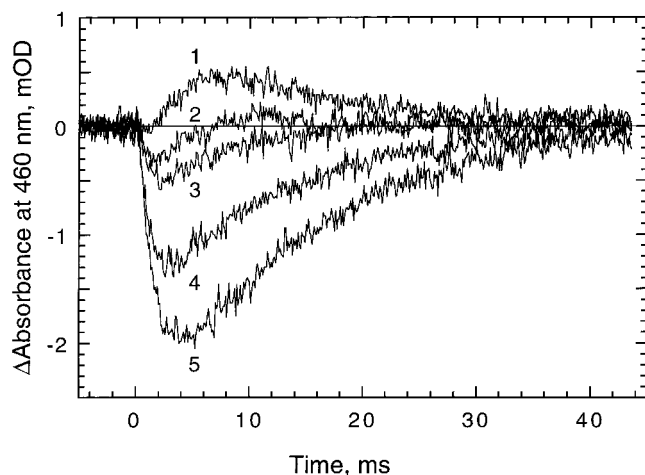


FIGURE 8: Light-induced absorption changes of the pH-sensitive dye pyranine in a suspension of R134H membranes at different pH values in 150 mM KCl. A decrease of absorbance is due to proton release into the suspension; an increase of absorbance is due to proton uptake. Traces 1–5 were taken at pH 6.0, 6.3, 6.5, 6.8, and 7.0.

the Ground State. In the WT bR at neutral pH, the proton release group releases a proton to the extracellular side almost coincident with the protonation of D85 from the Schiff base (13–16). The PRG consists of R82, E194, E204, and one or more water molecules. The short distance between the positively charged R134 and negatively charged E194 (Figure 1) implies that each may help to stabilize the other's pK_a . From the most recent structure of bR (11), two hydrogen bonds are assigned between R134 and the peptide carboxyl of E194 (Figure 1). Data shown above imply that R134 can affect the photocycle, indirectly, by interaction with E194, a part of the PRG. Replacing the arginine with a short side-chain residue, histidine, alters the interaction between these two residues, therefore affecting some characteristics of the photocycle.

The pH dependence of the rate constant of dark adaptation in R134H shows no major differences compared to that of the WT (see Table 1 and the inset in Figure 4). The titration curve can be fitted with two components as for the WT. Our interpretation for the complex titration curve is that the protonation of D85 is coupled with the deprotonation of another group, X (26, 28). In the R134H mutant, the pK_a of D85 when X is protonated is 2.9 (see Table 1 and the inset in Figure 4), which is a little higher than that in WT the (2.6). The coincidence between the acid titration curve and the dark adaptation curve in the low pH range confirms that the protonation of D85 increases the rate of dark adaptation (26). From these measurements, the pK_a of X in the unphotolyzed state is 9.8 in R134H (see Table 1 and the inset in Figure 4), but the alkaline titration of the transition into P480 suggests this pK_a may be around 8.9 (Figure 3). The source of the difference in these two estimates is not quite clear. It is possible that the pK_a of partial transformation of the pigment into P480 does not exactly coincide with the pK_a of the PRG.

The pK_a of the PRG in the unphotolyzed state can also be estimated from the pH dependence of M formation. M formation can be decomposed into two kinetic components, fast and slow. The amplitudes of these two components

depend on the concentrations of the forms of the initial pigment, one form having the PRG protonated and the pK_a of D85 being low, and the other form having the PRG deprotonated and the pK_a of D85 being high. The fast component of M formation in the WT and other mutants reflects the process of proton transfer from the Schiff base to D85 (2, 4, 19, 21). The amplitude of the fast component is controlled by the difference of the proton affinities between these two residues (19, 21). The slow component reflects the transition of M_1 to the next M substate. The amplitude of the fast component increases as the pH increases, at least partly because as the pH increases, the PRG changes from its protonated to its unprotonated state. This protonation change will in turn affect the pK_a of D85. The pK_a of D85 will increase several pK units when the PRG becomes deprotonated at high pH. This pK_a elevation reduces the pK_a difference between D85 and the Schiff base, therefore making proton transfer from the Schiff base to D85 easier at high pH. In the WT, the pK_a of the fraction of the M formation amplitude (fast and slow components) is 9.2 in 150 mM KCl (33). This pK_a shifts to 8.7 in this mutant. The one pK unit difference for the pK_a of the PRG measured with the two methods (9.8 in dark adaptation versus 8.7 in M) may be caused by the structural differences of bR in these two states (unphotolyzed state versus M state).

Origin of the pH Dependence of the Fraction of O and Its Connection with the pK_a of the PRG. When the pH decreases from 7.9 to 3.0, the fraction and lifetime of O increase, similar to those in the WT (27, 34, 35). We have suggested that the rate constant of the $O \rightarrow bR$ transition is controlled by the protonation state of the PRG (27); therefore, at low pH, when the PRG is protonated, deprotonation of D85 and O decay are slowed, which results in a larger O amplitude. The rate constant for O formation is pH independent below pH 7 (around 90 s^{-1} , Figure 7B), while the rate constant of O decay is pH dependent, dropping from 250 to 10 s^{-1} as the pH decreases from 6.8 to 2.5 in R134H. The rate constant of O decay has a pK_a of 5.0 or larger in R134H (see Table 1 and Figure 7B). Balashov et al. (27) have provided evidence that the pK_a of the rate constant of the $O \rightarrow bR$ transition represents the pK_a of the PRG in the O intermediate. Then the pK_a of the PRG in O for the R134H mutant is 5.0, which is 0.7 pK unit higher than in the WT (see Table 1). The pH dependence of the O amplitude and the rate constant of the $O \rightarrow bR$ transition in R134H are similar to those in the E194D mutant (27), indicating that perturbation of either of the two interacting residues causes similar changes. The relatively short distance between the polar groups of R134 and E194 (11) suggests that R134 may interact with E194 through a hydrogen bond and it may act as a counterion for E194. The replacement of R134 by another potentially positively charged residue, histidine, lifts the pK_a of the PRG about 0.7 pK unit compared to that in the WT. This is similar to what we observed in the E194D mutant (27). In both mutants, a long-chain, charged residue (E in E194D and R in R134H) was replaced by a shorter-chain, charged residue (D for E194 and H for R134). Both replacements would decrease the interaction between these two residues, thereby affecting the pK_a of the PRG. The second pK_a in the pH dependence of the O amplitude of this mutant is 6.4, one pK unit lower than that in the WT and E204Q and E194Q mutants (all about 7.2–7.5). The group

with a pK_a of 7.2 seen in the WT (27, 35–38) and the E204Q and E194Q mutants (27) was tentatively assigned to D96 in the late N or O states (27). The reason for the decreased pK_a (and decreased amount of O intermediate at neutral pH) in R134H as well as in E194D (27) should be investigated further. Our hypothesis is that it may reflect accelerated deprotonation and a decreased pK_a of D85 in the N and O intermediate in these mutants (27).

The pK_a of the PRG when the pigment is in the M state can be determined from the pH dependence of the light-induced fast proton release (19). The pK_a is the pH at which the order of the light-induced proton release and uptake is reversed. This pK_a was found to be 5.7 in 150 mM KCl in the WT (19). In R134H, the pK_a shifts to 6.3 (see Table 1 and Figure 8). At higher pH (pH > 6.3), proton release precedes the uptake, similar to that in the WT. At lower pH (pH < 6.3), the order of proton release and uptake is reversed, with proton uptake preceding proton release. The observation of a shift in the pK_a of fast proton release and alteration of the pH dependence of the rate constant of the O \rightarrow bR transition suggest that R134 affects the pK_a of the PRG during the photocycle, probably by its interaction with E194. The weaker interaction between H134 and E194 in R134H affects the pK_a of E194, D85, and other residues in PRG through the hydrogen bond and electrostatic interaction. The increase in the pK_a of the rate constant of the O \rightarrow bR transition in R134H and the large increase in the fraction of O at pH below 5 provides further evidence that deprotonation of D85 and the O \rightarrow bR transition are controlled by the protonation state of the PRG (27).

The replacement of R134 with a charged residue, lysine (21) or histidine (this work), causes relatively moderate changes in the pK_a values of D85 and the PRG and kinetics of the photocycle reactions. We found that much larger perturbations occur upon replacement of R134 with a neutral residue, cysteine. In the R134C mutant, the pK_a of D85 is increased to ca. 7 and the fast proton release is practically inhibited (39). This indicates the importance of the conserved residue R134 in maintaining the functional structure of the pigment (40) and an efficient photocycle.

REFERENCES

1. Ebrey, T. G. (1993) in *Thermodynamics of Membranes, Receptors and Channels* (Jackson, M., Ed.) pp 353–387, CRC Press, Boca Raton, FL.
2. Lanyi, J. K., and Váró, G. (1995) *Isr. J. Chem.* 35, 365–385.
3. *Photophysics and Photochemistry of Retinal Proteins* (Ottolenghi, M., and Sheves, M., Eds.) (1995) *Isr. J. Chem.* 34, 193–513.
4. Lanyi, J. K. (1999) *Int. Rev. Cytol.* 187, 161–202.
5. Brown, L. S., Sasaki, J., Kandori, H., Maeda, A., Needleman, R., and Lanyi, J. K. (1995) *J. Biol. Chem.* 270, 27122–27126.
6. Kandori, H., Yamazaki, Y., Hatanaka, M., Needleman, R., Brown, L. S., Richter, H.-T., Lanyi, J. K., and Maeda, A. (1997) *Biochemistry* 36, 5134–5141.
7. Govindjee, R., Misra, S., Balashov, S. P., Ebrey, T. G., Crouch, R. K., and Menick, D. R. (1996) *Biophys. J.* 71, 1011–1023.
8. Balashov, S. P., Imasheva, E. S., Ebrey, T. G., Chen, N., Brown, L. S., Richter, H.-T., Lanyi, J. K., and Crouch, R. K. (1997) *Biochemistry* 36, 8671–8676.
9. Dioumaev, A. K., Richter, H.-T., Brown, L. S., Tanio, M., Tuzi, S., Saito, H., Kimura, Y., Needleman, R., and Lanyi, J. K. (1998) *Biochemistry* 37, 2496–2506.
10. Rammelsberg, R., Huhn, G., Lübken, M., and Gerwert, K. (1998) *Biochemistry* 37, 5001–5009.
11. Luecke, H., Schobert, B., Richter, H.-T., Cartailler, J.-P., and Lanyi, J. K. (1999) *J. Mol. Biol.* 291, 899–911.
12. Luecke, H., Schobert, B., Richter, H.-T., Cartailler, J.-P., and Lanyi, J. K. (1999) *Science* 286, 255–260.
13. Heberle, J., and Dencher, N. A. (1992) *Proc. Natl. Acad. Sci. U.S.A.* 89, 5996–6000.
14. Cao, Y., Brown, L. S., Sasaki, J., Maeda, A., Needleman, R., and Lanyi, J. K. (1995) *Biophys. J.* 68, 1518–1530.
15. Alexiev, U., Mollaaghababa, R., Scherrer, P., Khorana, H. G., and Heyn, M. P. (1995) *Proc. Natl. Acad. Sci. U.S.A.* 92, 372–376.
16. Liu, S. Y., Kono, M. and Ebrey, T. G. (1991) *Biophys. J.* 60, 204–216.
17. Souvignier, G., and Gerwert, K. (1992) *Biophys. J.* 63, 1393–1405.
18. Dencher, N., and Wilms, M. (1975) *Biophys. Struct. Mech.* 1, 259–271.
19. Zimányi, L., Váró, G., Chang, M., Ni, B., Needleman, R., and Lanyi, J. K. (1992) *Biochemistry* 31, 8535–8543.
20. Balashov, S. P., Govindjee, R., Kono, M., Imasheva, E. S., Lukashev, E., Ebrey, T. G., Crouch, R. K., Menick, D. R. and Feng, Y. (1993) *Biochemistry* 32, 10331–10343.
21. Misra, S., Martin, C., Kwon, O., Ebrey, T. G., Chen, N., Crouch, R. K., and Menick, D. R., (1997) *Photochem. Photobiol.* 66, 774–783.
22. Grigorieff, N., Ceska, T. A., Downing, K. H., Baldwin, J. M., and Henderson, R. (1996) *J. Mol. Biol.* 259, 393–421.
23. Kimura, Y., Vassilyev, D. G., Miyazawa, A., Kidera, A., Matsushima, M., Mitsuoka, K., Murata, K., Hirai, T., and Fujiyoshi, Y. (1997) *Nature* 389, 206–211.
24. Essen, L. O., Siegert, R., Lehmann, W. D., and Oesterheld, D. (1998) *Proc. Natl. Acad. Sci. U.S.A.* 95, 11673–11678.
25. Belrhali, E., Nollert, P., Royant, A., Menzel, C., Rosenbusch, J. R., Landau, E. M., and Pebay-Peyroula, E. (1999) *Structure* 7, 909–917.
26. Balashov, S. P., Imasheva, E. S., Govindjee, R., and Ebrey, T. G. (1996) *Biophys. J.* 70, 473–481.
27. Balashov, S. P., M. Lu, Imasheva, E. S., Govindjee, R., Ebrey, T. G., Chen, Y. M., Othersen, B., III, Crouch, R. K., and Menick, D. R. (1999) *Biochemistry* 38, 2026–2039.
28. Balashov, S. P., Govindjee, R., Imasheva, E. S., Misra, S., Ebrey, T. G., Feng, Y., Crouch, R. K., and Menick, D. R. (1995) *Biochemistry* 34, 8820–8834.
29. Govindjee, R., Balashov, S. P., and Ebrey, T. G. (1990) *Biophys. J.* 58, 597–608.
30. Govindjee, R., Imasheva, E. S., Misra, S., Balashov, S. P., Ebrey, T. G., Chen, N., Menick, D. R., and Crouch, R. K. (1997) *Biophys. J.* 72, 886–898.
31. Subramaniam, S., Marti, T., and Khorana, H. G. (1990) *Proc. Natl. Acad. Sci. U.S.A.* 87, 1013–1017.
32. Metz, G., Siebert, F., and Engelhard, M. (1992) *FEBS Lett.* 303, 237–242.
33. Balashov, S. P., Govindjee, R., and Ebrey, T. G. (1991) *Biophys. J.* 60, 475–490.
34. Richter, H.-T., Needleman, R., Kandori, H., Maeda, A., and Lanyi, J. K. (1996) *Biochemistry* 35, 15461–15466.
35. Bressler, S., Friedman, N., Li, Q., Ottolenghi, M., Saha, C., and Sheves, M. (1999) *Biochemistry* 38, 2018–2025.
36. Li, Q., Govindjee, R., and Ebrey, T. G. (1984) *Proc. Natl. Acad. Sci. U.S.A.* 81, 7079–7082.
37. Einfeld, W., Pusch, C., Diller, R., Lohrmann, R., and Stockburger, M. (1993) *Biochemistry* 32, 7196–7215.
38. Cao, Y., Brown, L. S., Needleman, R., and Lanyi, J. K. (1993) *Biochemistry* 32, 10239–10248.
39. Lu, M., Balashov, S. P., Ebrey, T. G., Chen, N., Chen, Y., Menick, D. R., and Crouch, R. K. (1999) *Biophys. J.* 76, A241.
40. Feng, Y., Chen, N., Hazard, E. S., Misra, S., Ebrey, T. G., Menick, D. R., and Crouch, R. K. (1995) *Biophys. J.* 68, A334.